
A CONTINUAL DEEPFAKE DETECTION BENCHMARK: DATASET, METHODS, AND ESSENTIALS

**Chuang Li¹, Zhiwu Huang^{2,*}, Danda Pani Paudel¹, Yabin Wang³,
Mohamad Shahbazi¹, Xiaopeng Hong⁴ & Luc Van Gool^{1,5}**

¹ETH Zürich, Switzerland ²Singapore Management University, Singapore

³Xi'an Jiaotong University, China ⁴Harbin Institute of Technology, China

⁵KU Leuven, Belgium

chuqli@student.ethz.ch, zwhuang@smu.edu.sg

{paudel, mshahbazi, vangool}@vision.ee.ethz.ch,

iamwangyabin@stu.xjtu.edu.cn, hongxiaopeng@ieee.org

ABSTRACT

There have been emerging a number of benchmarks and techniques for the detection of deepfakes. However, very few works study the detection of incrementally appearing deepfakes in the real-world scenarios. To simulate the wild scenes, this paper suggests a continual deepfake detection benchmark (CDDDB) over a new collection of deepfakes from both known and unknown generative models. The suggested CDDDB designs multiple evaluations on the detection over easy, hard, and long sequence of deepfake tasks, with a set of appropriate measures. In addition, we exploit multiple approaches to adapt multiclass incremental learning methods, commonly used in the continual visual recognition, to the continual deepfake detection problem. We evaluate several methods, including the adapted ones, on the proposed CDDDB. Within the proposed benchmark, we explore some commonly known essentials of standard continual learning. Our study provides new insights on these essentials in the context of continual deepfake detection. The suggested CDDDB is clearly more challenging than the existing benchmarks, which thus offers a suitable evaluation avenue to the future research. Our benchmark dataset and the source code will be made publicly available.

1 INTRODUCTION

Most existing deepfake techniques use deep generative neural networks, such as autoencoders, generative adversarial nets (GANs) and generative normalizing flows (Glows), to generate visual fake images and videos as deepfakes. The development of these techniques enables us to generate high-realistic deepfakes that are indistinguishable from the real images and videos. As a result, there is a growing threat of “weaponizing” deepfakes for malicious purposes, which is potentially detrimental to privacy, society security and democracy Chesney & Citron (2019). To contend with this threat, a large number of deepfake detection datasets (e.g., Korshunov & Marcel (2018); Li et al. (2018; 2019b); Dufour & Gully (2019); Rossler et al. (2019); Dolhansky et al. (2020); Jiang et al. (2020)) and techniques (e.g., Zhou et al. (2017); Afchar et al. (2018); Yang et al. (2019); Nguyen et al. (2019b;a); Agarwal et al. (2019)) are proposed.

The primary focus of existing deepfake detection benchmark datasets and techniques is of stationary kind. In contrast, a vast variety of deepfakes are evolving day by day with the increasingly improved generative models. For instance, GANs have significantly evolved from vanilla GANs to the current state-of-the-art GANs (e.g., Karras et al. (2019); Ntavelis et al. (2022); Shahbazi et al. (2021; 2022)) which produce much more realistic-looking images. In turn, deepfake detectors trained on vanilla GANs are expected to perform poorly on the deepfakes from the state-of-the-art GANs. Therefore, learning continual deepfake detection (CDD) is highly desirable. However in current stage, the CDD benchmarks and the problem study remains fairly limited.

*Corresponding Author

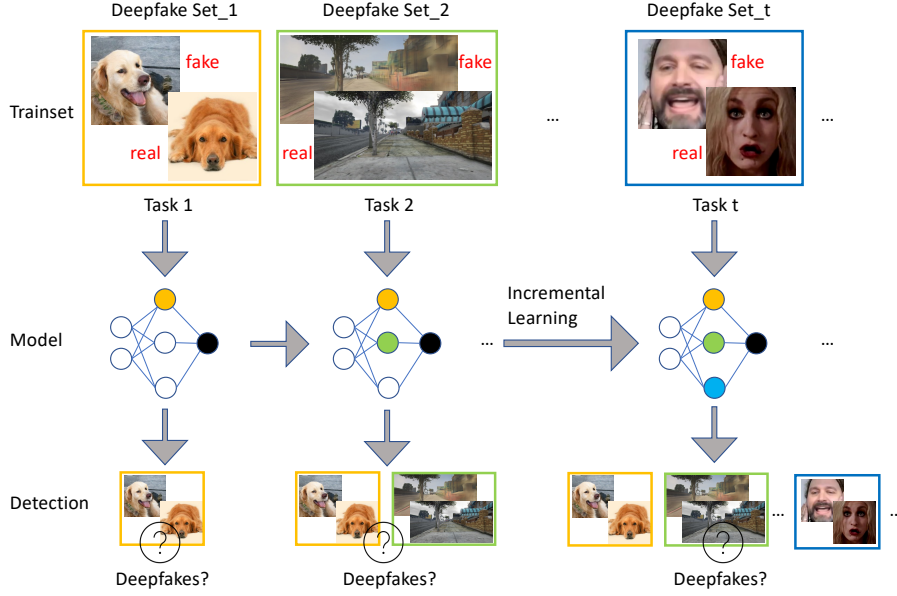


Figure 1: Continual deepfake detection (CDD) problem that aims at learning a unified model over incrementally occurring deepfake detection tasks without catastrophic forgetting on old deepfakes.

In this paper, we establish a challenging continual deepfake detection benchmark (CDDDB) by gathering publicly available deepfakes, from both known and unknown generative models. The CDDDB then gradually introduces deepfakes to simulate the real-world deepfakes’ evolution, as shown in Fig.1. The key benchmarking task is to measure whether the involved detectors are able to incrementally learn new deepfake detection tasks without forgetting old ones.

Up to our knowledge, there exist only two similar benchmarks Marra et al. (2019); Kim et al. (2021). Both of these benchmarks are limited as they merely perform CDD on only one deepfake type of known generative models (e.g., GANs or face-swap like deepfake models). As mentioned, the source of deepfakes may not only be unknown but also be of diverse types, in practice. Therefore, we proposed a new CDDDB which better resembles the real-world scenarios. Furthermore, our CDDDB also categorizes the evaluation protocol into different cases: from easy to hard and short to long CDD sequences. Such categorization allows us to better probe the CDD methods.

We evaluate seven well-known and most promising existing continual learning methods on our established benchmark. In this process, we first evaluate the existing multi-class incremental learning methods, commonly used in the continual visual recognition, in the CDD settings. Furthermore, we develop multiple approaches to adapt multiclass continual learning methods to the binary CDD problem. Our evaluations also include several other variants which are evaluated for easy/hard and short/long sequences. These exhaustive evaluations offer us two major benefits: (a) suitable baselines for the future CDD research; (b) new insights on the established continual learning essentials in the context of CDD. In the latter case, we explore some accepted essentials including (i) knowledge distillation; (ii) class imbalance issue; (iii) memory budget. Notably, our empirical evidence suggests that the existing consideration for class imbalance issues can be significantly hurtful to the CDD performance.

The major contributions of this paper can be summarized as follows:

- We propose a realistic and challenging continual deepfake detection dataset along with the evaluation protocols to thoroughly probe CDD methods.
- We evaluate several existing and adapted methods on the proposed benchmark. These evaluations serve as lock, stock, and barrel of CDD baselines.
- Using the proposed dataset and conducted evaluations, we study several aspects of CDD problem. Our study offers new insights on the CDD essentials.

Dataset	Real Source	Deepfake Source	Continual
Deepfake-TIMIT Korshunov & Marcel (2018)	VidTIMIT dataset Sanderson & Lovell (2009)	Known Deepfake tech	✗
UADFW Yang et al. (2019)	EBV dataset Li et al. (2018)	Known Deepfake tech	✗
FaceForensics++ Rossler et al. (2019)	YouTube	Known Deepfake tech	✗
Celab-DF v2 Li et al. (2020)	YouTube	Known Deepfake tech	✗
DFDC Dolhansky et al. (2020)	Actors	Known Deepfake tech	✗
WildDeepfake Zi et al. (2020)	Internet	Unknown Deepfake tech	✗
WhichFaceReal whi	Internet	Unknown Deepfake tech	✗
CNNfake Wang et al. (2020)	Multi-Datasets	Known Deepfake tech	✗
GANfake Marra et al. (2019)	Multi-Datasets	Known Deepfake tech	✓
CoReD* Kim et al. (2021)	Multi-Datasets	Known Deepfake tech	✓
CDDb (ours)	Multi-Datasets&Internet	Known&unknown tech	✓

Table 1: Comparison of prominent deepfake datasets. Only GANfake Marra et al. (2019), CoReD Kim et al. (2021) and our CDDb study continual fake detection benchmarks. However, both GANfake and CoReD merely detect pure GAN-generated images (or pure deepfake-generated videos), while ours studies a high mixture of deepfake sources, which are from either known generative models or unknown ones (i.e., directly from internet). CoReD* dataset is not publicly available.

2 RELATED WORK

Datasets and Benchmarks for Deepfake Detection. To evaluate deepfake detection methods, many datasets and benchmarks have been proposed. For instance, FaceForensic++ Rossler et al. (2019) contains face videos collected from YouTube and manipulated using deepfake dee, Face2Face Thies et al. (2016), Faceswap fac and Neural Texture Thies et al. (2019). WildDeepfake Zi et al. (2020) aims at real-world deepfakes detection by collecting real and fake videos with unknown source model directly from the internet. CNNfake Wang et al. (2020) proposes a diverse dataset obtained from various image synthesis methods, including GAN-based techniques (e.g., Karras et al. (2018), Brock et al. (2019)) and traditional deepfake methods. Table 1 summarizes the prominent benchmark datasets for deepfake detection. The majority of the proposed benchmarks do not include incremental detection in their experimental setup. While few works, namely GANfake Marra et al. (2019) and CoReD Kim et al. (2021), have addressed the CDD setting, they either only address known GAN-based deepfakes Marra et al. (2019) or only treat known GAN fakes and known traditional deepfakes separately Kim et al. (2021). Furthermore, their studied task sequences are generally short (e.g. they consist of 4 or 5 tasks). However, in the real-world scenario, deepfakes might come from known or unknown source models. These models might be based on GANs or traditional methods, and finally, they form a long sequence of tasks evolving through time. To bridge the gap between the current benchmarks and the real-world scenario, our proposed dataset includes a collection of deepfakes from both known or unknown sources. In addition, the suggested benchmark provides three different experimental setups (Easy, Hard, and Long) for a thorough evaluation of CDD methods.

Deepfake Detection Methods. Along with the discussed benchmarks, many approaches have been proposed for deepfake detection (e.g., Rossler et al. (2019); Li & Lyu (2018); Nguyen et al. (2019b); Afchar et al. (2018); Matern et al. (2019); Nguyen et al. (2019a); Marra et al. (2019); Wang et al. (2020)). These approaches mainly aim at finding generalizable features from a set of available samples that can be used to detect deepfakes at test time. For instance, Rossler et al. (2019) employs XceptionNet Chollet (2017), a CNN with separable convolutions and residual connections, pre-trained on ImageNet Deng et al. (2009) and fine-tuned for deepfake detection. Similarly, Wang et al. (2020) uses ResNet-50 He et al. (2016) pretrained with ImageNet, and further train it in a binary classification setting for deepfake detection. Different to the aforementioned methods, Marra et al. (2019) and Kim et al. (2021) address the continual adaptation of deepfake detection models to new sources while avoiding catastrophic forgetting (i.e. forgetting previous sources). To this end, they formulate the problem as an incremental learning process, where each new deepfake source is treated as a new task. Marra et al. (2019) adapts one of the traditional CIL methods, i.e., incremental classifier and representation learning (iCaRL) Rebuffi et al. (2017), through a multi-task learning

scheme over both deepfake recognition and detection tasks. To mitigate the catastrophic forgetting, Marra et al. (2019) keeps using the original iCaRL’s knowledge distillation loss, which enforces the newly updated network to output close prediction results to those of the network trained on the previous task given the same samples from an exemplar set of old samples. Similarly, CoReD Kim et al. (2021) tackles forward learning and backward forgetting with a student-teacher learning paradigm, where the teacher is the model trained for the previous tasks, and the student is the new model being adapted to also include the current task. CoReD does not store samples from previous tasks, as it only uses samples from the current task for the teacher-to-student knowledge distillation. To further mitigate the forgetting problem, the method adds a feature-level knowledge distillation loss (i.e., representation loss).

Class-incremental Learning (CIL). Many studies on continual visual recognition have explored different CIL methods. In this paper, we focus on three prominent categories: *gradient-based*, *memory-based* and *distillation-based*.¹

Gradient-based methods (e.g., Riemer et al. (2018); Zeng et al. (2019); Farajtabar et al. (2020); Saha et al. (2020); Tang et al. (2021); Wang et al. (2021)) overcome the catastrophic forgetting by minimizing the interference among task-wise gradients when updating network weights. For instance, Farajtabar et al. (2020) suggests storing a set of gradient directions in the memory of each task and alleviates forgetting by taking gradients in the orthogonal directions for new tasks. Similarly, Wang et al. (2021) proposes a null space class-incremental learning (NSCIL) method to train the network on the new task by projecting its gradient updates to the null space of the approximated covariance matrix on all the past task data.

Memory-based methods mitigate forgetting by either replaying a small set of examples from past tasks stored in a memory (rehearsal) Robins (1995); Rebuffi et al. (2017); Lopez-Paz & Ranzato (2017); Chaudhry et al. (2018); Hu et al. (2018); Kemker & Kanan (2018); Chaudhry et al. (2019) or replaying synthesized data from previous tasks using generative models (pseudo-rehearsal) Shin et al. (2017); van de Ven et al. (2021). For example, Rebuffi et al. (2017); Aljundi et al. (2019) explore ways of selecting small sets of exemplars from previous tasks, which can be replayed to the model when learning a new task. Instead of using raw old data, LRCIL Pellegrini et al. (2020) suggests to replay latent feature maps from intermediate layers of the model in order to reduce the required memory and computation.

Distillation-based methods (e.g., Li & Hoiem (2017); Rebuffi et al. (2017); Hou et al. (2019); Castro et al. (2018); Wu et al. (2019); Yu et al. (2020); Tao et al. (2020); Liu et al. (2020); Mittal et al. (2021)) apply knowledge distillation Hinton et al. (2015) to alleviate catastrophic forgetting. The key idea is applying a distillation loss between a network (teacher) trained on previous tasks and a network (student) being trained on current task to alleviate the performance degradation of the student on previous tasks. Some distillation-based methods can also be considered as memory-based, since they require exemplars from old data for the teacher. iCaRL Rebuffi et al. (2017) is one of these approaches, which improves exemplar selection needed for the distillation using a prioritized selection method based on herding, which selects samples closest to the sample means. Rebuffi et al. (2017) also identifies *class imbalance* as a crucial challenge for CMC, as they observe that the test samples are more likely to be classified as the new classes. To deal with this issue, Rebuffi et al. (2017) suggests a classification strategy named nearest-mean-of-exemplars. Following the same motivation, LUCIR Hou et al. (2019) learns a unified classifier via re-balancing, which is applying cosine normalization to the magnitude of the parameters in fully-connected (FC) layers, in order to eliminate the bias in the predictions toward new classes. More recently, Mittal et al. (2021) exploits a compositional learning paradigm to separate the learning on the new task data and the one on the exemplar set that contains equally-sized sets of both old and new samples.

Discussion. The discussed methods are mostly designed for multi-class incremental learning (CIL), which aims to learn a unified classifier for a set of sequentially-encountered classes. As Deepfake detection can be regarded as a binary task or a set of binary tasks Marra et al. (2019), we further investigate the different ways of adapting these methods to the problem of CDD on the suggested CDDDB.

¹There exist also methods based on regularization (e.g. Kirkpatrick et al. (2017); Zenke et al. (2017); Aljundi et al. (2018)) or expansion (e.g. Yoon et al. (2017); Lee et al. (2017); Hung et al. (2019)).

Family	Deepfake Source	Real Source	# Images
GAN Model	ProGAN Karras et al. (2018)	LSUN	736.0k
	StyleGAN Karras et al. (2019)	LSUN	12.0k
	BigGAN Brock et al. (2019)	ImageNet	4.0k
	CycleGAN Zhu et al. (2017)	Style/object transfer	2.6k
	GauGAN Park et al. (2019)	COCO	10.0k
	StarGAN Choi et al. (2018)	CelebA	16.8k
Non-GAN Model	Glow Kingma & Dhariwal (2018)	CelebA	16.8k
	CRN Chen & Koltun (2017)	GTA	12.8k
	IMLE Li et al. (2019a)	GTA	12.8k
	SAN Dai et al. (2019)	Standard SR benchmark	440
	FaceForensics++ Rossler et al. (2019)	YouTube	5.4k
Unknown Model	WildDeepfake Zi et al. (2020)	Internet	10.5k
	WhichFaceReal whi	Internet	2.0k

Table 2: A new collection of mixed deepfake sources for the suggested CDDB.

3 SUGGESTED BENCHMARK DATASET

To build a more real-world continual deepfake detection benchmark (CDDB) dataset, we collect a mixture of publicly available deepfakes and real sources from either known or unknown generative models. *We suggest keeping the dataset as an open set to include more new or future sources of real data and fake data, so that a real-world CDD scenario will be finally achieved.* On the new collection of deepfakes and reals, we suggest three evaluation scenarios as well as their corresponding evaluation metrics for more real-world CDD setups.

3.1 DATA COLLECTION

The new data collection comprises 3 families of deepfake sources: 1) GAN models, 2) non-GAN models, and 3) unknown generative models. Below details the deepfake sources and their associated real sources, which are listed in Table 2.

GAN Models. This family consists of fake images synthesized by 6 *GAN models*. ProGAN Karras et al. (2018) and StyleGAN Karras et al. (2019) are two of the most popular unconditional GANs. They were trained on each category of the dataset LSUN Yu et al. (2015) and thus they can produce realistic looking LSUN images. BigGAN Brock et al. (2019) is one of the state-of-the-art class-conditional GAN models trained on ImageNet Deng et al. (2009). Moreover, we include three image-conditional GAN models for image-to-image translation, namely CycleGAN Zhu et al. (2017), GauGAN Park et al. (2019) and StarGAN Choi et al. (2018). These models were trained on one style/object transfer task selected from the dataset collected by Zhu et al. (2017), COCO dataset Lin et al. (2014), and CelebA dataset Liu et al. (2015), respectively.

Non-GAN Models. This set further contains deepfake images generated by 8 *non-GAN models*, including Generative Flow model (Glow) Kingma & Dhariwal (2018), Cascaded Refinement Networks (CRN) Chen & Koltun (2017), Implicit Maximum Likelihood Estimation (IMLE) Li et al. (2019a), Second-order attention network (SAN) Dai et al. (2019) and 4 conventional deepfake models (Deepfake dee, Face2Face Thies et al. (2016), Faceswap fac and Neural Texture Thies et al. (2019)) from FaceForensics++ Rossler et al. (2019). These non-GAN generative models were trained on CelebA Liu et al. (2015), GTA Richter et al. (2016), a standard SR benchmark and YouTube videos, respectively, for high-fidelity image synthesis.

Unknown Models. This group includes deepfake images from 2 *unknown generative models*, one collected by WildDeepfake Zi et al. (2020) and one by WhichFaceReal whi. They both collect deepfakes and real images/videos directly from the internet. WildDeepfake Zi et al. (2020) originally contains deepfake/real videos. As our focus is on the detection of deepfake images, we randomly

select a number of frames from each video. This group of models are included to further simulate the real-world, where the source model of the encountered deepfakes might not be known.

3.2 EVALUATION SCENARIOS

From the proposed collection of deepfakes, a large number of differently-ordered sequences of tasks can be produced to study CDD. In our benchmark, we suggest three different evaluation scenarios: an easy task sequence (*EASY*), a hard task sequence (*HARD*), and a long task sequence (*LONG*). The *EASY* setup is used to study the basic behavior of evaluated methods when they address an easy CDD problem. The *HARD* setup aims to evaluate the performance of competing methods when facing a more challenging CDD problem. We generate this sequence by empirically observing their difficulties for CDD. The *LONG* setup is designed to encourage methods to better handle long sequences of Deepfake detection tasks, where the catastrophic forgetting becomes more serious. The three evaluation sequences are detailed as follows:

1. *EASY*: {GauGAN, BigGAN, CycleGAN, IMLE, FaceForensic++, CRN, WildDeepfake}
2. *HARD*: {GauGAN, BigGAN, WildDeepfake, WhichFaceReal, SAN}
3. *LONG*: {GauGAN, BigGAN, CycleGAN, IMLE, FaceForensic++, CRN, WildDeepfake, Glow, StarGAN, StyleGAN, WhichFaceReal, SAN}

As it is a common practice in CIL (e.g., Rebuffi et al. (2017); Hou et al. (2019); Tao et al. (2020); Mittal et al. (2021)), we allow pre-training the model on one base task (not from the evaluation sequence) as a warm-up step. Following Wang et al. (2020) we suggest pre-training every evaluated methods over the fake images of ProGAN and the corresponding real samples.

3.3 EVALUATION METRICS

Similar to traditional CMC problems, the CDD problem should also concentrate on studying the performance of the evaluated methods in terms of forward learning of each new task, as well as backward forgetting of previous ones. Accordingly, we suggest using the average detection accuracy (*AA*) and the average forgetting degree (*AF*), i.e., mean of backward transfer degradation (BWT) Lopez-Paz & Ranzato (2017), as the evaluation metrics. Formally, we can obtain a test accuracy matrix $B \in \mathbb{R}^{n \times n}$ (i.e., upper triangular matrix), where each entry $B_{i,j}$ indicates the test accuracy of the i -th task after training the j -th task and n is the total number of involved tasks. *AA* and *AF* can be calculated as $AA = \frac{1}{n} \sum_{i=1}^n B_{i,n}$, $AF = \frac{1}{n-1} \sum_{i=1}^{n-1} BWT_i$, where $BWT_i = \frac{1}{n-i-1} \sum_{j=i+1}^n (B_{i,j} - B_{i,i})$.

As CDD is a detection problem, we also suggest using mean average precision (*mAP*) to measure the performance of evaluated methods in terms of the trade-off between precision and recall, where we regard real samples as negatives and fake samples as positive. Each AP is defined as the area under the precision-recall (PR) curve for deepfake detection over one single deepfake task in the sequence Wang et al. (2020). *mAP* is the average of all the APs calculated over all detection tasks.

As different tasks may contain the same or similar real samples, and some fake samples could be from unknown generative models, we additionally employ the average deepfake recognition accuracy (*AA-M*) to study the challenge for identifying the specific deepfake and real resources. This metric is mainly used for understanding the gap between CMC and CBC.

4 PROPOSED BENCHMARKING METHODS

The studied CDD problem requires to distinguish real and fake samples from the sequentially occurring sources of real/fake pairs. If we regard each real/fake source as an independent class, the CDD problem can be relaxed to a CMC problem, that can be addressed by CIL system. Accordingly, this section focuses on studying three main adaptations of CIL to better address CDD on the CDDb.

4.1 PROBLEM DEFINITION AND OVERVIEW

In the CDD problem, DeepFakes sources and their corresponding real images appear sequentially in time, forming the sequence $\mathcal{X} = \{\mathcal{X}_1, \mathcal{X}_2 \dots, \mathcal{X}_t\}$, where $\mathcal{X}_i = (X_i^R, X_i^F)$ represents the paired

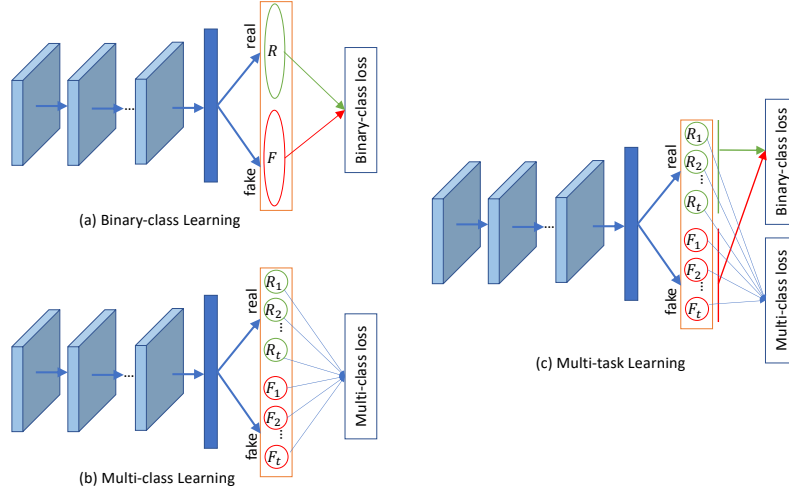


Figure 2: Three main adaptations (a), (b), (c) of multi-class incremental learning for CDD. Here R, F indicate the logits/features for reals and fakes respectively, and t is the number of deepfake tasks.

set of real and fake images corresponding to source i . At each incremental step t , complete data is only available for the new pair of real and fake image sets $\mathcal{X}_t = (X_t^R, X_t^F)$. For memory-based and distillation-based methods, we can additionally have a small amount of exemplar data $\mathcal{P} = \{\mathcal{P}_1, \mathcal{P}_2 \dots, \mathcal{P}_{t-1}\}$, which is selected from previous data $\mathcal{X} = \{\mathcal{X}_1, \mathcal{X}_2 \dots, \mathcal{X}_{t-1}\}$ for rehearsal or distillation. The trained models at step t are finally expected to distinguish all the fake and real images corresponding to the sources observed up to and including step t .

The problem can be relaxed to a CMC problem, once each real/fake source is regarded as an independent class. In this case, traditional CIL methods can be applied. A *basic CIL system* is to train a network model Θ that consists of a deep feature extractor $\phi(\cdot)$ and a fully-connected (FC) layer $f_c(x)$. Like a standard multi-class classifier, the output logits are processed through an activation function $\varphi(\cdot)$ before classification loss ℓ_{class} is evaluated corresponding to the correct class. To address the catastrophic forgetting, many of the state-of-the-art CIL methods generally apply distillation loss ℓ_{distill} over the exemplar set \mathcal{P} of old samples from previous tasks. In addition, a supplementary loss ℓ_{supp} is often applied to strengthen the classification over multiple classes at \mathcal{P} . In general, the loss function for CIL systems can be formulated as:

$$\ell_{\text{CIL}}(\Theta) = \ell_{\text{class}}(\mathcal{X}_t, \Theta) + \gamma_d \ell_{\text{distill}}(\mathcal{P}, \Theta) + \gamma_m \ell_{\text{supp}}(\mathcal{P}, \Theta) \quad (1)$$

where γ_d, γ_m are hyperparameters for the trade-off among the three losses. The classification loss is the usual cross-entropy loss calculated on the new data

$$\ell_{\text{class}}(\mathcal{X}_t, \Theta) = - \sum_{x_i \in \mathcal{X}_t} \sum_{y_j=1}^k \delta_{y_j=y_i} \log g_{y_j}(x_i) \quad (2)$$

where $\delta_{y_j=y_i}$ is an indicator to check whether the prediction y_j is in line with the ground truth y_i , k is the total class number, $g_{y_j}(\cdot) = \varphi(\cdot) \circ f_c(\cdot) \circ \phi(\cdot)$ is the classification score (probability) for the class y_j , and \circ is function composition. The distillation term, is the *KL-divergence* loss Hinton et al. (2015) with temperature T :

$$\ell_{\text{distill}}(\mathcal{P}, \Theta) = - \sum_{x_i \in \mathcal{P}} T^2 D_{KL}(g^T(x_i) || \tilde{g}^T(x_i)) \quad (3)$$

where $\tilde{g}(\cdot)$ is the old classifier, which is the one before the current updating phase. As done by Hou et al. (2019), the distillation can be also performed over the feature level, i.e. $\ell_{\text{distill}}(\mathcal{P}, \Theta) = - \sum_{x_i \in \mathcal{P}} 1 - \langle \tilde{\phi}(x_i), \phi(x_i) \rangle$, where $\tilde{\phi}(\cdot), \phi(\cdot)$ are the feature extractors of the old and new networks respectively, and $\langle \cdot \rangle$ denotes cosine similarity. The additional term could be a margin ranking loss from Hou et al. (2019):

$$\ell_{\text{supp}}(\mathcal{P}, \Theta) = \sum_{x_i \in \mathcal{P}} \sum_{y_j=1}^J \max(\tau - \langle \theta^{y_i}, \phi(x_i) \rangle + \langle \theta^{y_j}, \phi(x_i) \rangle, 0) \quad (4)$$

where $\langle \cdot \rangle$ indicates cosine similarity, τ is the margin threshold, θ is class embeddings (i.e., weight parameterization of the FC layer), θ^{y_i} is the ground truth class embedding of x_i , θ^{y_j} is one of the nearest- J class embeddings. The loss pushes nearest classes away from the given class.

The three losses can be also applied to different data. For example, ℓ_{class} and ℓ_{distill} can be also used to simultaneously learn over both the new and old data, i.e., $\mathcal{P} \cup \mathcal{X}_t$. In this paper, we mainly study three representative methods LRCIL Pellegrini et al. (2020), iCaRL Rebuffi et al. (2017) and LUCIR Pellegrini et al. (2020), all of which can be formulated by Eqn.1. For LRCIL, γ_d and γ_m are zeros. For iCaRL, γ_m is zero. By comparison, LUCIR applies non-zero γ_d and γ_m . *In this paper, we mainly focus on the necessary adaptations of the CIL objective (especially ℓ_{class}) required for effective CDD.*

4.2 ADAPTING CIL TO CDD

We study three main adaptations of CIL methods for CDD. This will help us to bridge the gap between CMC and CBC, and hence it allows for more solid benchmarking on the suggested CDD with a good reference to the CMC performances. The key idea for the adaption is to enforce the classification loss ℓ_{class} and the distillation loss ℓ_{distill} to better fit the binary classification (i.e., detection) task, which is formulated as

$$\ell_{\text{BIL}}(\Theta) = \hat{\ell}_{\text{class}}(\mathcal{X}_t, \Theta) + \gamma_d \hat{\ell}_{\text{distill}}(\mathcal{P}, \Theta) + \gamma_m \ell_{\text{supp}}(\mathcal{P}, \Theta) \quad (5)$$

where $\hat{\ell}_{\text{class}}$ and $\hat{\ell}_{\text{distill}}$ are the main adapted components. Below details three main ways for the adaption on them.

Binary-class (BC) Learning. One of the most straightforward solutions (Fig.2 (a)) is to change the categorical cross-entropy loss with the binary one:

$$\hat{\ell}_{\text{class}}(\mathcal{X}_t, \Theta) = - \sum_{x_i \in \mathcal{X}_t} \delta_{y=y_i} \log g_y(x_i) + (1 - \delta_{y=y_i}) \log(1 - g_y(x_i)) \quad (6)$$

where $\delta_{y=y_i}$ is an indicator for the ground-truth label y_i , $g_y(x_i)$ applies Sigmoid function $\varphi(x_i)$ instead, calculating the probability of the given sample x_i being a fake sample. In addition, the distillation loss $\hat{\ell}_{\text{distill}}$ is based on the binary prediction. For the final classification, we apply the Sigmoid function based results. As ℓ_{supp} is originally designed for better multi-class classification, it can be ignored in the binary adaptation.

Multi-class (MC) Learning. For this approach (Fig.2 (b)), we use the original classification, distillation, and supplementary losses, i.e. $\hat{\ell}_{\text{class}} = \ell_{\text{class}}$, $\hat{\ell}_{\text{distill}} = \ell_{\text{distill}}$, $\hat{\ell}_{\text{supp}} = \ell_{\text{supp}}$. We regard each real/fake class from different tasks as an independent class. For classification, we apply $\hat{y}_i = \arg \max_{y_j} g_{y_j}(x_i)$, given a sample x_i . If \hat{y}_i is one of the fake/real classes, we will predict x_i to fake/real.

Multi-task (MT) Learning. Another soft adaption (Fig.2 (c)) is to apply a multi-task learning formulation. In particular, both the multi-class classification and the binary-class classification (i.e., the detection) tasks are managed by the same classifier $g(\cdot)$. To this end, we adapt the classification loss by adding a binary cross-entropy term to the categorical cross-entropy

$$\hat{\ell}_{\text{class}}(\mathcal{X}_t, \Theta) = (1 - \lambda) \ell_{\text{class}}(\mathcal{X}_t, \Theta) + \lambda \ell'_{\text{class}}(\mathcal{X}_t, \Theta) \quad (7)$$

where ℓ_{class} is the regular multi-class classification task loss Eqn.2, the binary-class classification task loss ℓ'_{class} is computed by taking into account the activations, $g(\cdot)$, of all the classes, separately for the fake and real classes, and the hyperparameter λ is for the balance between these two task-based losses. Formally, ℓ'_{class} is computed by

$$\ell'_{\text{class}}(\mathcal{X}_t, \Theta) = \sum_{x_i \in (\mathcal{X}_t)} \delta_{Y=F} d_F(x_i) + \delta_{Y=R} d_R(x_i) \quad (8)$$

where $d_F(x_i)$ and $d_R(x_i)$ are designed for the aggregation over all fake classes and all real classes respectively. In this paper, we study the following four aggregation approaches: (1) *SumLog* (Eqn.9a) that is proposed in Marra et al. (2019), (2) *SumLogit* (Eqn.9b), (3) *SumFeat* (Eqn.9c),

Learning System	Evaluated Method	CDDb-EASY1500							AA	AF	AA-M	mAP
		Task1	Task2	Task3	Task4	Task5	Task6	Task7				
Backbone	CNNDetWang et al. (2020)- Pretrain	63.85	68.75	71.95	60.93	91.31	60.93	49.01	66.68	NA	NA	79.02
	CNNDetWang et al. (2020)- Finetune	57.25	51.00	57.63	47.81	80.41	48.00	78.77	60.28	-14.29	NA	61.67
Binary-class (BC) learning	NSCILWang et al. (2021)- Sigmoid*	48.35	50.25	49.43	56.58	56.56	70.73	57.63	55.65	-42.04	NA	63.50
	LRCILPellegrini et al. (2020)- Sigmoid*	83.00	88.00	82.82	96.20	79.02	97.14	62.82	<u>84.14</u>	-9.15	NA	<u>91.37</u>
	iCaRLRebuffi et al. (2017)- Sigmoid*	76.90	80.00	88.93	99.41	85.03	99.45	76.64	<u>87.05</u>	-10.64	NA	<u>92.25</u>
	LUCIRHou et al. (2019)- Sigmoid*	90.60	91.05	90.46	99.80	91.04	99.80	75.38	<u>91.16</u>	-4.76	NA	<u>95.94</u>
Multi-class (MC) learning	NSCILWang et al. (2021)	46.80	52.50	47.90	45.26	35.21	51.33	58.85	48.26	-50.88	8.41	44.26
	LRCILPellegrini et al. (2020)	83.50	77.88	90.84	98.90	84.75	98.86	65.92	<u>85.81</u>	-5.88	67.11	<u>92.63</u>
	iCaRLRebuffi et al. (2017)	77.50	71.38	91.22	99.57	95.66	99.92	78.28	<u>87.65</u>	-9.41	65.39	<u>94.12</u>
	LUCIRHou et al. (2019)- LinFC	91.60	89.12	92.56	99.76	94.45	99.80	71.21	<u>91.21</u>	-2.88	74.62	<u>94.75</u>
Multi-task (MT) learning	CCILMittal et al. (2021)- LinFC	60.50	66.12	81.49	96.16	73.38	98.55	60.45	76.66	-16.50	41.85	86.29
	LRCILPellegrini et al. (2020)- SumLogMarra et al. (2019)	86.65	85.63	91.79	99.22	88.72	99.57	68.27	<u>88.76</u>	-3.99	66.03	<u>93.95</u>
	iCaRLRebuffi et al. (2017)- SumLogMarra et al. (2019)	74.40	78.38	88.36	99.65	92.24	99.69	79.84	<u>87.05</u>	-10.72	71.41	<u>93.02</u>
	LUCIRHou et al. (2019)- SumLogMarra et al. (2019)	88.70	88.62	93.89	99.37	94.82	99.80	75.71	<u>91.56</u>	-3.65	74.47	<u>95.47</u>
	LRCILPellegrini et al. (2020)- SumLogit	86.95	88.12	92.75	99.45	88.35	99.45	70.24	<u>89.33</u>	-4.27	68.00	<u>94.84</u>
	iCaRLRebuffi et al. (2017)- SumLogit	85.25	86.12	88.93	99.65	92.98	99.80	80.27	<u>90.43</u>	-6.12	74.18	<u>95.27</u>
	LUCIRHou et al. (2019)- SumLogit	89.95	89.62	94.47	99.65	95.75	99.80	74.79	<u>92.00</u>	-3.13	73.55	<u>95.26</u>
	LRCILPellegrini et al. (2020)- SumFeat	84.85	85.13	92.56	99.26	87.15	99.45	69.90	<u>87.81</u>	-5.30	66.40	<u>93.73</u>
	iCaRLRebuffi et al. (2017)- SumFeat	77.90	84.25	90.84	99.65	82.72	99.69	79.11	<u>87.74</u>	-9.52	68.15	<u>93.88</u>
	LUCIRHou et al. (2019)- SumFeat	90.05	89.38	94.85	99.92	95.01	99.92	73.53	<u>91.81</u>	-3.12	74.23	<u>95.66</u>
	LRCILPellegrini et al. (2020)- Max	87.80	89.00	92.18	67.96	87.15	99.22	69.85	<u>89.16</u>	-4.43	69.38	<u>94.60</u>
	iCaRLRebuffi et al. (2017)- Max	82.35	87.00	92.94	99.76	91.77	99.73	79.74	<u>89.92</u>	-6.79	73.47	<u>94.87</u>
	LUCIRHou et al. (2019)- Max	89.85	91.25	94.08	99.53	92.51	99.65	72.61	<u>91.21</u>	-4.00	74.06	<u>95.41</u>
Joint Training	CNNDetWang et al. (2020)- Binary	98.65	98.38	96.37	100.00	95.19	100.00	79.59	95.20	NA	NA	98.36
	CNNDetWang et al. (2020)- Multi	95.70	97.00	95.80	99.96	96.30	99.96	75.28	94.29	NA	79.28	97.25

Table 3: Benchmarking results on the suggested CDDb’s *EASY* evaluation. Sigmoid*: applying Sigmoid function based classification loss. AA: Average Accuracy for deepfake detection, AF: Average Forgetting degree, AA-M: Average Accuracy for deepfake recognition, mAP: mean Average Precision. The AAs and mAPs of the evaluated methods (i.e., LRCIL, iCaRL, LUCIR) are in **green**, **blue**, and **red** respectively. **Bold**: best **green/blue/red** results, Underline: second best **green/blue/red** results.

and (4) *Max* (Eqn.9d).

$$d_F(x_i) = \sum_{y \in \{fake\}} \log g_y(x_i), \quad d_R(x_i) = \sum_{y \in \{real\}} \log g_y(x_i) \quad (9a)$$

$$d_F(x_i) = \log \sum_{y \in \{fake\}} g_y(x_i), \quad d_R(x_i) = \log \sum_{y \in \{real\}} g_y(x_i) \quad (9b)$$

$$d_F(x_i) = \log g_y \left(\sum_{y \in \{fake\}} x_i \right), \quad d_R(x_i) = \log g_y \left(\sum_{y \in \{real\}} x_i \right) \quad (9c)$$

$$d_F(x_i) = \max_{y \in \{fake\}} (\log g_y(x_i)), \quad d_R(x_i) = \max_{y \in \{real\}} (\log g_y(x_i)) \quad (9d)$$

where $y \in \{fake\}$ indicates all the associated fake classes, and $y \in \{real\}$ corresponds to all the real classes.

For the MT case, we use the original distillation and supplementary losses, i.e. $\hat{\ell}_{\text{distill}} = \ell_{\text{distill}}$, $\hat{\ell}_{\text{supp}} = \ell_{\text{supp}}$, where ℓ_{distill} and ℓ_{supp} are computed using Eqn.3 and Eqn.4, respectively. As done in the multi-class learning case, we use $\hat{y}_i = \arg \max_{y_j} g_{y_j}(x_i)$ for the final classification.

Learning System	Evaluated Method	CDDB-EASY1500							AA	AF	AA-M
		Task1	Task2	Task3	Task4	Task5	Task6	Task7			
Multi-class (MC) learning	LRCILPellegrini et al. (2020)	83.50	77.88	90.84	98.90	84.75	98.86	65.92	85.81	-5.88	67.11
	LUCIR(CosFC)Hou et al. (2019)	81.05	88.25	94.47	99.73	90.30	99.73	57.15	87.24	-10.32	71.42
	CCIL(CosFC)Mittal et al. (2021)	55.65	56.88	67.18	89.34	75.88	89.38	64.32	71.23	-22.01	39.53
	LRCILPellegrini et al. (2020)-KD	86.25	79.88	94.85	99.06	81.15	99.22	67.57	86.85	-5.50	66.57
	LUCIRHou et al. (2019)-LinFC	91.60	89.12	92.56	99.76	94.45	99.80	71.21	91.21	-2.88	95.41
	CCILMittal et al. (2021)-LinFC	60.50	66.12	81.49	96.16	73.38	98.55	60.45	76.66	-16.50	41.85

Table 4: Evaluation results on essentials of CIL methods on CDDB’s *EASY* evaluation. AA: Average Accuracy for detection, AF: Average Forgetting degree, AA-M: Average Accuracy for recognition. The AA results of LRCIL, LUCIR, CCIL are in green, red, and brown respectively.

5 BENCHMARKING RESULTS

We evaluate three families of CIL methods with our exploited variants (using BC, MC, MT) on the suggested CDDB for the three scenes (Sec.3.2): 1) *EASY*, 2) *HARD*, and 3) *LONG*, with the introduced measures (Sec.3.3). The three sets of state-of-the-art CIL methods are: 1) Gradient-based: null space class incremental learning (NSCIL) Wang et al. (2021), 2) Memory-based: latent replay class incremental learning (LRCIL), and 3) Distillation-based: incremental classifier and representation learning (iCaRL) Rebuffi et al. (2017), Learning a Unified Classifier Incrementally via Rebalancing (LUCIR) Hou et al. (2019), Compositional Class Incremental Learning (CCIL). Besides, we evaluated the multi-task variant of iCaRL (iCaRL-SumLog)² Marra et al. (2019). For a fair comparison, we employ the state-of-the-art deepfake CNN detector (CNNDet) Wang et al. (2020) that applies a ResNet-50 pretrained on ImageNet Deng et al. (2009) and ProGAN Karras et al. (2018) as the backbone for all the evaluated methods over the proposed CDDB. For most of the methods, we used their official codes, and tuned their hyperparameters for better performances. For a consistency, we empirically set the MT learning hyperparameter as $\lambda = 0.3$ for all the MT methods. For *EASY*, *HARD* and *LONG*, we assign the same memory budget (i.e., 1500) for all those methods that need a memory to save exemplars. Additionally, we study two reduced memory budgets (i.e., 1000, 500) for *HARD*. For all the evaluations, we evaluate the joint training methods using CNNDet with binary classification loss (CNNDet-Binary) and multiclass classification loss (CNNDet-Multi) to study the approximated upper bound for the incremental learning methods. The detailed settings and the parameter studies are presented in the suppl. material³.

5.1 EASY EVALUATION

Table 3 reports the benchmarking results of the evaluated methods for the CDDB *EASY*. Table 4 studies other essential components for the CDD problem.

Basic Findings on Essentials. 1) Due to the serious forgetting problem, *finetuning* the CNNDet method works worse than the pretrained CNNDet model over ProGAN. 2) The clearly inferior performances of the *state-of-the-art gradient-based method NSCIL* might be because its null space cannot be approximated well on the highly heterogeneous fakes and reals. 3) LRCIL merely performs a rehearsal on the data to address forgetting, and thus we added a *knowledge distillation* (KD) term to LRCIL (i.e., LRCIL-KD), which further improves AA with a marginally worse AA-M. (see Table 4). 4) The *state-of-the-art distillation-based method CCIL* does not work well. From Table 4, we discover that its used cosine normalization based fully connected layer (CosFC) Hou et al. (2019) clearly hurts the performance (see the comparison LUCIR-CosFC vs. LUCIR-LinFC, CCIL-CosFC vs. CCIL-LinFC in Table 4). Thus, we replace CosFC with regular FC (LinFC) in both LUCIR and CCIL for better performances. Despite the replacement, we find that CCIL’s intrinsic separate Softmax also leads to remarkably inferior performance, by comparing CCIL-LinFC against LRCIL-KD in Table 4. This is because their major difference is one uses combined softmax for old and new samples, and the other one uses separated softmax for old and new samples. Both CosFC and separated softmax were proposed to address the *class imbalance issue*, with which the test samples are often predicted into new classes in the CMC context. However, predicting the test fakes into the new fake class is acceptable for our studied CDD problem. Therefore, the two hard normalization/separation techniques are very likely to hurt the CDD performance.

²We overlooked the existing method Kim et al. (2021), as its code was not available before the submission.

³The supp. metrial also studies GANfake Marra et al. (2019). As it does not release the detailed train/val/test splits, we can only empirically study our own splits following the description in the oiriginal paper.

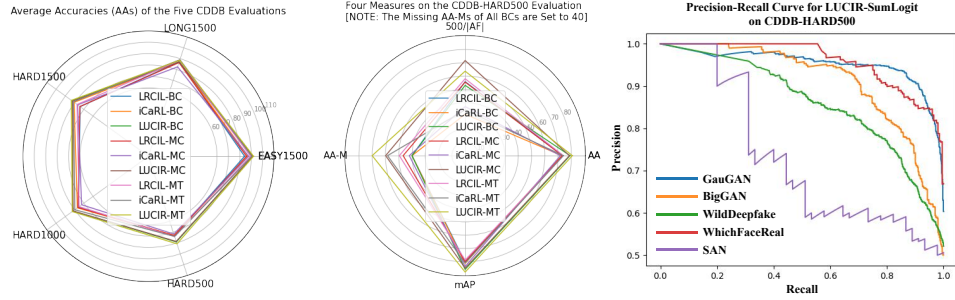


Figure 3: **Left:** Radar plot (the bigger covering area the better) on AAs of the evaluated methods for CDDB’s *EASY1500*, *LONG1500*, *HARD1500*, *HARD1000*, *HARD500*. **Middle:** Radar plot on AAs, AFs, mAPs and AA-Ms of the evaluated methods for *HARD500*. **Right:** Precision-recall (PR) curves of LUCIR-SumLogit with the highest mAP for *HARD500*. HARDm: HARD with memory budget= m , BC/MC/MT: binary-class/multi-class/multi-task learning methods that have the highest AAs/mAPs, AA: Average Accuracy (detection), AF: Average Forgetting degree, AA-M: Average Accuracy (recognition), mAP: mean Average Precision, i.e., the mean of areas under the PR curve.

Learning System	Evaluated Method	CDDB-HARD1500				CDDB-LONG1500			
		AA	AF	AA-M	mAP	AA	AF	AA-M	mAP
Binary-class (BC) learning	LRCIL Pellegrini et al. (2020)- Sigmoid*	<u>74.07</u>	-5.43	NA	<u>80.40</u>	<u>87.06</u>	-4.79	NA	<u>91.81</u>
	iCaRL Rebuffi et al. (2017)- Sigmoid*	<u>80.52</u>	-7.89	NA	<u>87.76</u>	<u>87.12</u>	-6.92	NA	<u>91.68</u>
	LUCIR Hou et al. (2019)- Sigmoid*	<u>83.17</u>	-4.45	NA	<u>89.72</u>	<u>87.19</u>	-6.91	NA	<u>92.11</u>
Multi-class (MC) learning	LRCIL Pellegrini et al. (2020)	<u>74.22</u>	-5.41	57.74	<u>80.21</u>	<u>86.40</u>	-4.65	62.32	<u>91.28</u>
	iCaRL Rebuffi et al. (2017)	<u>76.72</u>	-7.79	67.46	<u>85.05</u>	<u>82.50</u>	-10.76	53.49	<u>89.63</u>
	LUCIR Hou et al. (2019)- LinFC	<u>82.33</u>	-3.12	66.27	<u>86.73</u>	<u>86.95</u>	-6.77	69.74	<u>91.43</u>
Multi-task (MT) learning	LRCIL Pellegrini et al. (2020)- SumLogit	<u>77.28</u>	-2.70	60.22	<u>81.38</u>	<u>87.93</u>	-2.99	65.60	<u>92.45</u>
	iCaRL Rebuffi et al. (2017)- SumLogit	<u>81.16</u>	-7.84	69.00	<u>90.22</u>	<u>88.68</u>	-5.12	70.51	<u>93.10</u>
	LUCIR Hou et al. (2019)- SumLogit	<u>83.42</u>	-3.28	65.31	<u>87.89</u>	<u>88.57</u>	-5.78	71.55	<u>92.83</u>
	LRCIL Pellegrini et al. (2020)- Max	<u>76.93</u>	-2.55	59.20	<u>81.20</u>	<u>88.49</u>	-2.64	65.67	<u>92.49</u>
	iCaRL Rebuffi et al. (2017)- Max	<u>81.28</u>	-8.95	60.64	<u>88.61</u>	<u>89.05</u>	-5.24	71.35	<u>94.03</u>
Joint Training	LUCIR Hou et al. (2019)- SumFeat	<u>82.14</u>	-2.90	65.59	<u>87.39</u>	<u>88.40</u>	-5.30	70.99	<u>92.70</u>
	CNNDet Wang et al. (2020)-Binary	85.29	NA	NA	91.34	93.17	NA	NA	94.69
	CNNDet Wang et al. (2020)-Multi	84.63	NA	70.59	90.10	92.30	NA	78.71	94.82

Table 5: Benchmarking results on CDDB’s *HARD* and *LONG*. AA: Average detection Accuracy, AF: Average Forgetting, AA-M: Average Accuracy for recognition. mAP: mean Average Precision. **green:** LRCIL, **blue:** iCaRL, **red:** LUCIR. **Bold:** best results, Underline: second best results.

BC vs. MC vs. MT Learning Systems. Except for the case on LRCIL, we find that the BC variants of the rest models (like iCaRL and LUCIR) perform very comparably with their corresponding MC models in terms of AA and AF, showing that the fine-grained classes of the known/unknown resources are good for the detection. It also is good for the MC method to eventually label an image as a fake if the classifier decides for any of the fake classes. By comparison, most of the MT variants of LRCIL, iCaRL and LUCIR work better than (or at least comparable with) their corresponding BC and MC models in terms of AA, and some of MTs perform clearly better than their corresponding MCs in terms of AA-M. This mainly stems from the natural complementary properties between the fine-grained multi-class separation and the coarse-grained binary-class cohesion, and most of the suggested MT methods balance them well.

SumLog vs. SumLogit vs. SumFeat vs. Max. From Table 3, we can see that the *SumLogit* and *Max* variants mostly work better than the original *SumLog* Marra et al. (2019) for the two main measures, i.e., AA and mAP. This is mainly because of consistency with final classifier’s operation, which applies *argmax* to the resulting logits. By comparison, the *SumFeat* variants merely perform better than the original *SumLog* for LUCIR in terms of AA and mAP. This might be because, different from LRCIL and iCaRL, it additionally applies the metric learning like loss (i.e., margin ranking loss) and thus the resulting features might be more discriminative for the aggregation to address the binary classification.

5.2 HARD AND LONG EVALUATIONS

We select the top-2 BC, MC and MT models in terms of AA for LRCIL, iCaRL and LUCIR from the *EASY* evaluation for benchmarking *HARD* and *LONG*.

		Reduced Memory Budgets for CDDb-HARD							
Learning System	Evaluated Method	1000				500			
		AA	AF	AA-M	mAP	AA	AF	AA-M	mAP
Binary-class (BC) learning	LRCIL Pellegrini et al. (2020)- Sigmoid*	<u>75.61</u>	-6.35	NA	<u>80.30</u>	<u>73.51</u>	-8.96	NA	<u>80.36</u>
	iCaRL Rebuffi et al. (2017)- Sigmoid*	<u>76.99</u>	-10.28	NA	<u>85.46</u>	<u>72.91</u>	-16.01	NA	<u>81.34</u>
	LUCIR Hou et al. (2019)- Sigmoid*	<u>81.75</u>	-6.12	NA	<u>88.46</u>	<u>78.99</u>	-9.43	NA	<u>85.81</u>
Multi-class (MC) learning	LRCIL Pellegrini et al. (2020)	<u>76.39</u>	-4.39	55.10	<u>80.45</u>	<u>73.18</u>	-9.01	46.69	<u>79.90</u>
	iCaRL Rebuffi et al. (2017)	<u>72.37</u>	-13.04	41.43	<u>85.25</u>	<u>71.75</u>	-13.52	42.07	<u>83.61</u>
	LUCIR Hou et al. (2019)- LinFC	<u>81.57</u>	-3.09	65.96	<u>85.97</u>	<u>78.57</u>	-6.97	59.87	<u>84.87</u>
Multi-task (MT) learning	LRCIL Pellegrini et al. (2020)- SumLogit	<u>75.14</u>	-3.53	56.31	<u>81.05</u>	<u>73.05</u>	-9.08	49.99	<u>80.71</u>
	iCaRL Marra et al. (2019)- SumLogit	<u>79.76</u>	-8.73	66.66	<u>87.75</u>	<u>73.98</u>	-14.50	58.44	<u>81.00</u>
	LUCIR Hou et al. (2019)- SumLogit	<u>82.53</u>	-5.34	72.00	<u>88.14</u>	<u>79.70</u>	-8.18	65.86	<u>88.08</u>
	LRCIL Pellegrini et al. (2020)- Max	<u>74.52</u>	-5.18	43.65	<u>81.39</u>	<u>74.01</u>	-8.62	49.59	<u>78.72</u>
	iCaRL Marra et al. (2019)- Max	<u>78.55</u>	-8.69	65.34	<u>86.78</u>	<u>73.70</u>	-14.65	58.85	<u>81.06</u>
	LUCIR Hou et al. (2019)- SumFeat	<u>82.35</u>	-4.76	71.22	<u>88.93</u>	<u>80.77</u>	-7.85	70.03	<u>87.84</u>

Table 6: Benchmarking results on reduced memories for the suggested CDDb’s *HARD* evaluation. **green**: LRCIL, **blue**: iCaRL, **red**: LUCIR. **Bold**: best results, Underline: second best results.

EASY vs. HARD vs. LONG. As the LONG evaluation includes both easy and hard tasks, the evaluated methods generally get higher scores than the HARD evaluation. Besides, LONG’s overall AAs and mAPs are visibly worse than those on EASY, meaning that incremental learning over a longer sequence is more challenging. Interestingly, the AFs are not clearly worse, showing the forgetting issue is not serious in this context. By comparison, HARD’s overall AAs, mAPs and AA-Ms are clearly lower than those of EASY and LONG, because it contains more challenging deepfake tasks such as WildDeepfake, WhichFaceReal that are from the wild scenes and SAN that merely has a small data for training.

Memory Budget. As all the evaluated methods require a memory to utilize an exemplar set of old samples to address the forgetting problem, we evaluate the performance as a function of the memory budget. Table 6 summarizes the results for the HARD evaluation with memory budget being 1000 and 500. The results again demonstrates the suggested MTs mostly outperform their competitors in terms of AA, mAP, AA-M. The LUCIR-SumLogit and LUCIR-SumFeat generally performs the best. The memory reduction from 1500 to 500 result in clear drops in the terms of AAs, AA-Ms, AFs and mAPs, showing the memory budget is one of the most essential factors for the CDD problem.

Overall Spotlight. Fig.3 shows a radar plot of the five CDDb evaluations in terms of AAs, and a radar plot and PR curves of the HARD500 evaluations in terms of the suggested four measures (i.e., AAs, AFs, mAP, AA-Ms). Using the same or more advanced distillation-based CIL variants, the highest AA on HARD (i.e., around 80%, memory size=500) is clearly lower than those on the other two CDD benchmarks, i.e., GANfake Marra et al. (2019) and CoReD Kim et al. (2021), on which the highest AAs are above 96% (memory budget=512) and 86% (memory budget=0) respectively. The major challenge is due to the suggested CDDb on the collection of mixed known and unknown deepfakes, whereas they proposed performing CDD on either pure GAN-generated fakes or pure traditional deepfake-produced images. Besides, the rest three measures (i.e., AFs, mAP, AA-Ms) are overlooked by the two benchmarks, which however are valuable to study CDD. The low scores on them further imply that the suggested CDDb is challenging and thus will open up promising directions for more solid research on the CDD problem.

6 CONCLUSION AND OUTLOOK

The continual deepfake detection benchmark proposed in this paper attempts to bring attention to the real world problem of detecting evolving deepfakes. In this front, difficult cases of deepfakes, long-term aspects of continual learning, and the varieties of deepfake sources are considered. To invite novel solutions, their evaluation protocols and several baseline methods are established by borrowing the most promising ones from the literature. The proposed dataset, evaluation protocol, and established baselines will allow researchers to quickly test their creative ideas and probe them against the existing ones. Additionally, through our evaluations, we are able to provide empirical study to analyze and discuss the common practices of continual learning in the context of the CDD problem.

Our experimental results show that the proposed CDDb is significantly more challenging than the existing datasets, i.e., GANfake Marra et al. (2019) and CoReD Kim et al. (2021). Hence we believe it will open up promising new directions of solid research on continual deepfake detection. As future

works, other essentials remain to be studied, including 1) exemplar selection, 2) knowledge distillation, and 3) data augmentation. Due to the nature of the suggested CDDb, we recommend using the new collection of deepfakes as an open set. Accordingly, we welcome external contributions to include any newly appeared deepfake resources with the benchmark to simulate the real-world scenarios.

ACKNOWLEDGMENTS

This work was supported by the Singapore Ministry of Education (MOE) Academic Research Fund (AcRF) Tier 1 grant (MSS21C002). This work was also supported in part by the ETH Zürich Fund (OK), a Huawei gift, an Amazon AWS grant, and an Nvidia GPU grant. The authors would like to thank Ankush Panwar for processing the WildDeepFake dataset.

REFERENCES

- Deepfakes github. <https://github.com/deepfakes/faceswap>.
- Deepfakes faceswap github repository. <https://github.com/MarekKowalski/FaceSwap>.
- Which face is real? <http://www.whichfaceisreal.com>.
- Darius Afchar, Vincent Nozick, Junichi Yamagishi, and Isao Echizen. Mesonet: a compact facial video forgery detection network. In *WIFS*. IEEE, 2018.
- Shruti Agarwal, Hany Farid, Yuming Gu, Mingming He, Koki Nagano, and Hao Li. Protecting world leaders against deep fakes. In *CVPR workshops*, 2019.
- Rahaf Aljundi, Francesca Babiloni, Mohamed Elhoseiny, Marcus Rohrbach, and Tinne Tuytelaars. Memory aware synapses: Learning what (not) to forget. In *ECCV*, 2018.
- Rahaf Aljundi, Min Lin, Baptiste Goujaud, and Yoshua Bengio. Gradient based sample selection for online continual learning. *arXiv preprint arXiv:1903.08671*, 2019.
- Andrew Brock, Jeff Donahue, and Karen Simonyan. Large scale GAN training for high fidelity natural image synthesis. 2019.
- Francisco M Castro, Manuel J Marín-Jiménez, Nicolás Guil, Cordelia Schmid, and Karteek Alahari. End-to-end incremental learning. In *ECCV*, 2018.
- Arslan Chaudhry, Marc’Aurelio Ranzato, Marcus Rohrbach, and Mohamed Elhoseiny. Efficient lifelong learning with a-gem. *arXiv preprint arXiv:1812.00420*, 2018.
- Arslan Chaudhry, Marcus Rohrbach, Mohamed Elhoseiny, Thalaiyasingam Ajanthan, Puneet Kumar Dokania, Philip HS Torr, and Marc’Aurelio Ranzato. Continual learning with tiny episodic memories. *arXiv preprint arXiv:1902.10486*, 2019.
- Qifeng Chen and Vladlen Koltun. Photographic image synthesis with cascaded refinement networks. In *ICCV*, 2017.
- Bobby Chesney and Danielle Citron. Deep fakes: A looming challenge for privacy, democracy, and national security. *Calif. L. Rev.*, 107:1753, 2019.
- Yunjey Choi, Minje Choi, Munyoung Kim, Jung-Woo Ha, Sunghun Kim, and Jaegul Choo. Stargan: Unified generative adversarial networks for multi-domain image-to-image translation. In *CVPR*, 2018.
- François Chollet. Xception: Deep learning with depthwise separable convolutions. In *CVPR*, 2017.
- Tao Dai, Jianrui Cai, Yongbing Zhang, Shu-Tao Xia, and Lei Zhang. Second-order attention network for single image super-resolution. In *CVPR*, 2019.
- Jia Deng, Wei Dong, Richard Socher, Li-Jia Li, Kai Li, and Li Fei-Fei. Imagenet: A large-scale hierarchical image database. In *CVPR*, 2009.

-
- Brian Dolhansky, Joanna Bitton, Ben Pfau, Jikuo Lu, Russ Howes, Menglin Wang, and Cristian Canton Ferrer. The deepfake detection challenge (dfdc) dataset. *arXiv preprint arXiv:2006.07397*, 2020.
- Nick Dufour and Andrew Gully. Contributing data to deepfake detection research. *Google AI Blog*, 2019.
- Mehrdad Farajtabar, Navid Azizan, Alex Mott, and Ang Li. Orthogonal gradient descent for continual learning. In *AISTATS*, 2020.
- Kaiming He, Xiangyu Zhang, Shaoqing Ren, and Jian Sun. Deep residual learning for image recognition. In *CVPR*, 2016.
- Geoffrey Hinton, Oriol Vinyals, Jeff Dean, et al. Distilling the knowledge in a neural network. *arXiv preprint arXiv:1503.02531*, 2015.
- Saihui Hou, Xinyu Pan, Chen Change Loy, Zilei Wang, and Dahua Lin. Learning a unified classifier incrementally via rebalancing. In *CVPR*, 2019.
- Wenpeng Hu, Zhou Lin, Bing Liu, Chongyang Tao, Zhengwei Tao, Jinwen Ma, Dongyan Zhao, and Rui Yan. Overcoming catastrophic forgetting for continual learning via model adaptation. In *ICLR*, 2018.
- Ching-Yi Hung, Cheng-Hao Tu, Cheng-En Wu, Chien-Hung Chen, Yi-Ming Chan, and Chu-Song Chen. Compacting, picking and growing for unforgetting continual learning. *NeurIPS*, 2019.
- Liming Jiang, Ren Li, Wayne Wu, Chen Qian, and Chen Change Loy. Deepforensics-1.0: A large-scale dataset for real-world face forgery detection. In *CVPR*, 2020.
- Tero Karras, Timo Aila, Samuli Laine, and Jaakko Lehtinen. Progressive growing of GANs for improved quality, stability, and variation. In *ICLR*, 2018.
- Tero Karras, Samuli Laine, and Timo Aila. A style-based generator architecture for generative adversarial networks. In *CVPR*, 2019.
- Ronald Kemker and Christopher Kanan. Fearnnet: Brain-inspired model for incremental learning. In *ICLR*, 2018.
- Minha Kim, Shahroz Tariq, and Simon S Woo. Cored: Generalizing fake media detection with continual representation using distillation. In *ACMMM*, 2021.
- Durk P Kingma and Prafulla Dhariwal. Glow: Generative flow with invertible 1x1 convolutions. *NeurIPS*, 2018.
- James Kirkpatrick, Razvan Pascanu, Neil Rabinowitz, Joel Veness, Guillaume Desjardins, Andrei A Rusu, Kieran Milan, John Quan, Tiago Ramalho, Agnieszka Grabska-Barwinska, et al. Overcoming catastrophic forgetting in neural networks. *Proceedings of the national academy of sciences*, 114(13):3521–3526, 2017.
- Pavel Korshunov and Sébastien Marcel. Deepfakes: a new threat to face recognition? assessment and detection. *arXiv preprint arXiv:1812.08685*, 2018.
- Sang-Woo Lee, Jin-Hwa Kim, Jaehyun Jun, Jung-Woo Ha, and Byoung-Tak Zhang. Overcoming catastrophic forgetting by incremental moment matching. *NeurIPS*, 30, 2017.
- Ke Li, Tianhao Zhang, and Jitendra Malik. Diverse image synthesis from semantic layouts via conditional imle. In *ICCV*, 2019a.
- Yuezun Li and Siwei Lyu. Exposing deepfake videos by detecting face warping artifacts. *arXiv preprint arXiv:1811.00656*, 2018.
- Yuezun Li, Ming-Ching Chang, and Siwei Lyu. In ictu oculi: Exposing ai created fake videos by detecting eye blinking. In *WIFS*, 2018.

-
- Yuezun Li, Xin Yang, Pu Sun, Honggang Qi, and Siwei Lyu. Celeb-df: A new dataset for deepfake forensics. *onikle.com*, 2019b.
- Yuezun Li, Xin Yang, Pu Sun, Honggang Qi, and Siwei Lyu. Celeb-df: A large-scale challenging dataset for deepfake forensics. In *CVPR*, 2020.
- Zhizhong Li and Derek Hoiem. Learning without forgetting. *IEEE transactions on pattern analysis and machine intelligence*, 40(12):2935–2947, 2017.
- Tsung-Yi Lin, Michael Maire, Serge Belongie, James Hays, Pietro Perona, Deva Ramanan, Piotr Dollár, and C Lawrence Zitnick. Microsoft coco: Common objects in context. In *ECCV*, 2014.
- Yaoyao Liu, Yuting Su, An-An Liu, Bernt Schiele, and Qianru Sun. Mnemonics training: Multi-class incremental learning without forgetting. In *CVPR*, 2020.
- Ziwei Liu, Ping Luo, Xiaogang Wang, and Xiaoou Tang. Deep learning face attributes in the wild. In *ICCV*, 2015.
- David Lopez-Paz and Marc’Aurelio Ranzato. Gradient episodic memory for continual learning. *NIPS*, 2017.
- Francesco Marra, Cristiano Saltori, Giulia Boato, and Luisa Verdoliva. Incremental learning for the detection and classification of gan-generated images. In *WIFS*, 2019.
- Falko Matern, Christian Riess, and Marc Stamminger. Exploiting visual artifacts to expose deep-fakes and face manipulations. In *WACV Workshops*, 2019.
- Sudhanshu Mittal, Silvio Galesso, and Thomas Brox. Essentials for class incremental learning. In *CVPR*, 2021.
- Huy H Nguyen, Fuming Fang, Junichi Yamagishi, and Isao Echizen. Multi-task learning for detecting and segmenting manipulated facial images and videos. *arXiv preprint arXiv:1906.06876*, 2019a.
- Huy H Nguyen, Junichi Yamagishi, and Isao Echizen. Use of a capsule network to detect fake images and videos. *arXiv preprint arXiv:1910.12467*, 2019b.
- Evangelos Ntavelis, Mohamad Shahbazi, Iason Kastanis, Radu Timofte, Martin Danelljan, and Luc Van Gool. Arbitrary-scale image synthesis. In *CVPR*, 2022.
- Taesung Park, Ming-Yu Liu, Ting-Chun Wang, and Jun-Yan Zhu. Semantic image synthesis with spatially-adaptive normalization. In *CVPR*, 2019.
- Lorenzo Pellegrini, Gabriele Graffieti, Vincenzo Lomonaco, and Davide Maltoni. Latent replay for real-time continual learning. In *IROS*, 2020.
- Sylvestre-Alvise Rebuffi, Alexander Kolesnikov, Georg Sperl, and Christoph H Lampert. icarl: Incremental classifier and representation learning. In *CVPR*, 2017.
- Stephan R Richter, Vibhav Vineet, Stefan Roth, and Vladlen Koltun. Playing for data: Ground truth from computer games. In *ECCV*, 2016.
- Matthew Riemer, Ignacio Cases, Robert Ajemian, Miao Liu, Irina Rish, Yuhai Tu, and Gerald Tesauro. Learning to learn without forgetting by maximizing transfer and minimizing interference. *arXiv preprint arXiv:1810.11910*, 2018.
- Anthony Robins. Catastrophic forgetting, rehearsal and pseudorehearsal. *Connection Science*, 7(2): 123–146, 1995.
- Andreas Rossler, Davide Cozzolino, Luisa Verdoliva, Christian Riess, Justus Thies, and Matthias Nießner. Faceforensics++: Learning to detect manipulated facial images. In *ICCV*, 2019.
- Gobinda Saha, Isha Garg, and Kaushik Roy. Gradient projection memory for continual learning. In *ICLR*, 2020.

-
- C. Sanderson and B.C. Lovell. Multi-region probabilistic histograms for robust and scalable identity inference. *Lecture Notes in Computer Science*, 2009.
- Mohamad Shahbazi, Zhiwu Huang, Danda Pani Paudel, Ajad Chhatkuli, and Luc Van Gool. Efficient conditional gan transfer with knowledge propagation across classes. In *CVPR*, 2021.
- Mohamad Shahbazi, Martin Danelljan, Danda Pani Paudel, and Luc Van Gool. Collapse by conditioning: Training class-conditional GANs with limited data. In *ICLR*, 2022.
- Hanul Shin, Jung Kwon Lee, Jaehong Kim, and Jiwon Kim. Continual learning with deep generative replay. *arXiv preprint arXiv:1705.08690*, 2017.
- Christian Szegedy, Vincent Vanhoucke, Sergey Ioffe, Jon Shlens, and Zbigniew Wojna. Rethinking the inception architecture for computer vision. In *CVPR*, 2016.
- Shixiang Tang, Dapeng Chen, Jinguo Zhu, Shijie Yu, and Wanli Ouyang. Layerwise optimization by gradient decomposition for continual learning. In *CVPR*, 2021.
- Xiaoyu Tao, Xinyuan Chang, Xiaopeng Hong, Xing Wei, and Yihong Gong. Topology-preserving class-incremental learning. In *ECCV*, 2020.
- Justus Thies, Michael Zollhofer, Marc Stamminger, Christian Theobalt, and Matthias Nießner. Face2face: Real-time face capture and reenactment of rgb videos. In *CVPR*, 2016.
- Justus Thies, Michael Zollhöfer, and Matthias Nießner. Deferred neural rendering: Image synthesis using neural textures. *ACM Transactions on Graphics (TOG)*, 38(4):1–12, 2019.
- Gido M van de Ven, Zhe Li, and Andreas S Tolias. Class-incremental learning with generative classifiers. In *CVPR*, 2021.
- Sheng-Yu Wang, Oliver Wang, Richard Zhang, Andrew Owens, and Alexei A Efros. CNN-generated images are surprisingly easy to spot... for now. In *CVPR*, 2020.
- Shipeng Wang, Xiaorong Li, Jian Sun, and Zongben Xu. Training networks in null space of feature covariance for continual learning. In *CVPR*, 2021.
- Yue Wu, Yinpeng Chen, Lijuan Wang, Yuancheng Ye, Zicheng Liu, Yandong Guo, and Yun Fu. Large scale incremental learning. In *CVPR*, 2019.
- Xin Yang, Yuezun Li, and Siwei Lyu. Exposing deep fakes using inconsistent head poses. In *ICASSP*, 2019.
- Jaehong Yoon, Eunho Yang, Jeongtae Lee, and Sung Ju Hwang. Lifelong learning with dynamically expandable networks. *arXiv preprint arXiv:1708.01547*, 2017.
- Fisher Yu, Ari Seff, Yinda Zhang, Shuran Song, Thomas Funkhouser, and Jianxiong Xiao. Lsun: Construction of a large-scale image dataset using deep learning with humans in the loop. *arXiv preprint arXiv:1506.03365*, 2015.
- Lu Yu, Bartłomiej Twardowski, Xialei Liu, Luis Herranz, Kai Wang, Yongmei Cheng, Shangling Jui, and Joost van de Weijer. Semantic drift compensation for class-incremental learning. In *CVPR*, 2020.
- Guanxiong Zeng, Yang Chen, Bo Cui, and Shan Yu. Continual learning of context-dependent processing in neural networks. *Nature Machine Intelligence*, 1(8):364–372, 2019.
- Friedemann Zenke, Ben Poole, and Surya Ganguli. Continual learning through synaptic intelligence. In *ICML*, 2017.
- Peng Zhou, Xintong Han, Vlad I Morariu, and Larry S Davis. Two-stream neural networks for tampered face detection. In *CVPR Workshops*, 2017.
- Jun-Yan Zhu, Taesung Park, Phillip Isola, and Alexei A Efros. Unpaired image-to-image translation using cycle-consistent adversarial networks. In *ICCV*, 2017.
- Bojia Zi, Minghao Chang, Jingjing Chen, Xingjun Ma, and Yu-Gang Jiang. Wilddeepfake: A challenging real-world dataset for deepfake detection. In *ACMMM*, 2020.

A SUPPLEMENTARY MATERIAL

In the supplementary material, we further present (1) training details of the evaluated methods on the proposed continual deepfake detection benchmark (CDDDB), (2) study on more essential components of class incremental learning (CIL) methods on the suggested CDDDB, (3) evaluation on the GANFake Marra et al. (2019) dataset, and (4) more overviews of the suggested five CDDDB evaluations.

A.1 TRAINING SETTINGS

We evaluated three types of the state-of-the-art class incremental learning (CIL) methods on the suggested CDDDB.

Gradient-based Method. We used the official code of the null space class incremental learning method (NSCIL) Wang et al. (2021), which is one of the state-of-the-art gradient-based methods. We followed the official code’s setup to tune the hyperparameter λ from the default setup $\{10, 30\}$ to the new settings $\{100, 1\}$, which is used to select the smallest singular values corresponding to the null space. The larger λ leads to larger approximate null space, increasing the plasticity to learn new tasks while decreasing the memorization of old tasks Wang et al. (2021). We trained the NSCIL model for 12 epochs in total, as we found that training more epochs for NSCIL resulted in performance degradation. The initial learning rate is 0.001 for the first task and 0.0001 for all other tasks and is divided by 2 after 4 and 8 epochs for the EASY evaluation. For batch normalization layers, the learning rate starts from 5×10^{-5} . The other parameters are the same as official NSCIL implementation.

Memory-based Method. We employed latent replay class incremental learning (LRCIL) Pellegrini et al. (2020), which is one of the most effective and efficient memory-based methods. LRCIL was trained in the NSCIL’s framework, with 20 epochs in total, the initial learning rate is 0.001 for the first task and 0.0001 for all other tasks and is divided by 2 after 10 and 15 epochs for the EASY, HARD, LONG evaluations. For batch normalization layers, the learning rate starts from 5×10^{-5} . For the GANfake evaluation, we used 60 epochs instead and the initial learning rate is divided by 2 after 20 and 40 epoch. Following original LRCIL’s implementation, there is no knowledge distillation loss. We also tried to add distillation loss with a factor $\gamma_d = 0.3$. And we chose the second layer as latent layer. We used Adam with the batch size 32 to train the network.

Distillation-based Method. We utilized three state-of-the-art distillation-based methods, i.e., incremental classifier and representation learning (iCaRL) Rebuffi et al. (2017), Learning a Unified Classifier Incrementally via Rebalancing (LUCIR) Hou et al. (2019), Compositional Class Incremental Learning (CCIL) Mittal et al. (2021). Besides, we also evaluated the multi-task variant of iCaRL (iCaRL-SumLog) Marra et al. (2019).

For iCaRL, we trained its model for 30 epochs in total. The learning rate starts from 0.0001 and is divided by $\frac{10}{3}$ after 10 and 20 epochs for the EASY, HARD and LONG evaluations. For GANfake sequences, we used 60 epochs instead and the initial learning rate 0.001 is divided by $\frac{10}{3}$ after 20 and 40 epoch. Following the original iCaRL’s implementation, γ_d was set to 1 for knowledge distillation loss $\ell_{distill}$ with temperature as $T = 1$. We used Adam with the batch size 32 to train the network. For CCIL, we used its official code. The initial learning rate, total epoches and learning rate decay are the same as iCaRL. We tried the method with ($\gamma_d = 0.3$) or without ($\gamma_d = 0$) knowledge distillation $\ell_{distill}$. Also, we tried it with or without applying mixup and label smoothing techniques to the whole training process which is different from the original implementation (only for the first training phase), and we followed the relevant parameters (e.g. mixup weight). We used Adam with the batch size 32 to train the network. The other parameters are the same as the official implementation of CCIL.

For LUCIR, the learning rate starts from 0.0001 and is divided by 10 after 16 and 33 epochs (50 epochs in total) for the LONG evaluation. For the EASY, HARD and GANfake evaluations, we used 40 epochs and the learning rate is divided by 10 after 13 and 26 epoch. γ_d is set to 0.5 for knowledge distillation loss $\ell_{distill}$. γ_m was set to 0.1 for supplementary loss ℓ_{supp} . Within ℓ_{supp} , the number of closest class embeddings J was set to 2 and the threshold τ was set to 0.2 for all experiments. The other parameters are the same as official LUCIR implementation. We used Adam with the batch size 32 to train the LUCIR network.

Learning System	Evaluated Method	CDDB-EASY1500				
		0.1	0.3	0.5	0.7	0.9
Multi-task (MT) learning	LRCILPellegrini et al. (2020)- SumLogMarra et al. (2019)	89.54	88.76	86.51	87.08	87.20
	iCaRLRebuffi et al. (2017)- SumLogMarra et al. (2019)	88.97	87.05	87.51	87.39	86.29
	LUCIRHou et al. (2019)- SumLogMarra et al. (2019)	91.65	91.56	92.05	91.39	91.08
	LRCILPellegrini et al. (2020)- SumLogit	89.38	89.33	88.08	88.52	87.71
	iCaRLRebuffi et al. (2017)- SumLogit	88.52	90.43	90.37	87.88	87.57
	LUCIRHou et al. (2019)- SumLogit	91.48	92.00	91.90	91.11	91.67
	LRCILPellegrini et al. (2020)- SumFeat	88.23	87.81	88.33	87.68	86.27
	iCaRLRebuffi et al. (2017)- SumFeat	87.37	87.74	86.26	86.52	85.46
	LUCIRHou et al. (2019)- SumFeat	91.75	91.81	91.03	91.28	91.48
	LRCILPellegrini et al. (2020)- Max	89.17	89.16	87.83	88.27	85.66
	iCaRLRebuffi et al. (2017)- Max	90.11	89.92	89.76	90.78	87.11
	LUCIRHou et al. (2019)- Max	91.30	91.21	91.20	91.35	91.04

Table 7: Empirical study on different multi-task learning trade-off parameter λ values for the suggested CDDB’ EASY1500 evaluation. The reported results are Average Accuracies (AA) for continual deepfake detection. **Bold**: best **green/blue/red** results, Underline: second/third best **green/blue/red** results. The best/second-best/third-best LRCIL, iCaRL, LUCIR results are in **green**, **blue**, and **red** respectively. *Note that we aim at comparing all the colorized triplets (LRCIL, iCaRL, LUCIR)’s performances to see which triplets consistently perform well. Each triplet should be of the same MT variant and the same λ value.*

For a fair comparison, we used deepfake CNN detector (CNNDet) Wang et al. (2020) that applies a ResNet-50 pretrained on ImageNet Deng et al. (2009) and ProGAN Karras et al. (2018) as the network backbone for all the evaluated methods. For the multi-task (MT) learning variants of the evaluated CIL methods, the study on the trade-off hyperparameter λ is presented in Table 7. In Table 7, we aim to compare all the colorized triplets (LRCIL, iCaRL, LUCIR)’s performances to see which triplets consistently perform well. Each triplet should be of the same MT variant and the same λ value (e.g., LRCIL-SumLogit-0.3, iCaRL-SumLogit-0.3, LUCIR-SumLogit-0.3). By comparing these triplets in terms of their average performances on (LRCIL, iCaRL, LUCIR), we can see that the SumLogit case ($\lambda = 0.3$) works the most promisingly on the CDDB-EASY1500 evaluation. Furthermore, it is not feasible to tune the hyperparameters on the test data in the real-world scenario. Accordingly, we used the same hyperparameter $\lambda = 0.3$ for all the MT variants of LRCIL, iCaRL and LUCIR throughout the main paper.

A.2 STUDY ON MORE ESSENTIALS

Table 8 studies more essentials in CIL on CDDB. They are *cosine normalization* on linear fully connected (FC) layer, *label smoothing* and *mixup* techniques.

Linear FC (LinFC). The main paper finds that performing cosine normalization on FC (CosFC) layers result in LUCIR Hou et al. (2019) and CCIL Mittal et al. (2021) is clearly inferior performance than using LinFC. This is because CosFC is originally designed to address the *class imbalance issue*, which however is much less serious in the CDD context. We additionally apply LinFC to CCIL* Mittal et al. (2021) that further drops knowledge distillation. We can see that the LinFC version of CCIL* also performs better than its corresponding CosFC version, enhancing the conclusion that CosFC is too hard for class imbalance based normalization so that it really hurts the CDD performance.

Label Smoothing (LabelSM). We also study *LabelSM* that is commonly used to improve generalization and reduce overconfidence of classification models Szegedy et al. (2016); Mittal et al. (2021). This technique affects the cross-entropy loss for classification by interpolating the one-hot labels with a uniform distribution over the possible classes Mittal et al. (2021). From the results in Table 8, we can discover that LabelSM slightly improves the AA scores in the cases of iCaRL Re-

Learning System	Evaluated Method	CDDB-EASY1500							AA	AF	AA-M
		Task1	Task2	Task3	Task4	Task5	Task6	Task7			
Multi-class (MC) learning	LRCILPellegrini et al. (2020)	83.50	77.88	90.84	98.90	84.75	98.86	65.92	85.81	-5.88	67.11
	iCaRLRebuffi et al. (2017)	77.50	71.38	91.22	99.57	95.66	99.92	78.28	87.65	-9.41	65.39
	LUCIR(CosFC)Hou et al. (2019)	81.05	88.25	94.47	99.73	90.30	99.73	57.15	87.24	-6.32	63.27
	CCIL(CosFC)Mittal et al. (2021)	55.65	56.88	67.18	89.34	75.88	89.38	64.32	71.23	-22.01	39.53
	CCIL*(CosFC)Mittal et al. (2021)	58.35	60.00	71.37	86.25	90.48	86.21	71.01	74.81	-22.56	48.66
	LUCIRHou et al. (2019)- LinFC	91.60	89.12	92.56	99.76	94.45	99.80	71.21	91.21	-2.88	74.62
	CCILMittal et al. (2021)- LinFC	60.50	66.12	81.49	96.16	73.38	98.55	60.45	76.66	-16.50	41.85
	CCIL*Mittal et al. (2021)- LinFC	62.70	70.75	82.63	98.51	90.76	99.80	75.42	82.94	-13.24	61.95
	LRCILPellegrini et al. (2020)- LabelSM	72.70	74.13	89.89	99.45	92.14	99.57	72.52	85.77	-5.93	68.17
	iCaRLRebuffi et al. (2017)- LabelSM	79.55	80.62	90.46	99.84	89.37	99.84	80.17	88.55	-8.93	71.82
	LUCIRHou et al. (2019)- LabelSM	84.15	85.75	94.47	100.00	93.25	100.00	82.36	91.42	-5.31	77.35
	CCIL*Mittal et al. (2021)- LabelSM	58.60	65.25	61.83	98.43	88.54	98.43	72.52	77.66	-18.16	53.85
	LRCILPellegrini et al. (2020)- Mixup	52.30	52.13	62.40	85.54	78.65	96.94	70.00	71.14	-25.91	35.43
	iCaRLRebuffi et al. (2017)- Mixup	78.05	84.88	94.47	100.00	94.09	100.00	80.47	90.28	-6.95	75.42
	LUCIRHou et al. (2019)- Mixup	82.31	87.22	90.70	96.32	92.98	93.21	70.59	87.62	-6.54	70.93
	CCIL*Mittal et al. (2021)- Mixup	57.80	66.25	80.34	98.63	72.27	98.9	73.92	78.30	-18.98	55.16

Table 8: Benchmarking results on essentials of CIS methods on CDDB’s *EASY* evaluation. CCIL* indicates the CCIL method without using knowledge distillation loss. AA: Average Accuracy for deepfake detection, AF: Average Forgetting degree, AA-M: Average Accuracy for deepfake recognition. The AA results of LRCIL, iCaRL, LUCIR, CCIL are in green, blue, red, and brown respectively.

Learning System	Evaluated Method	GANfake Marra et al. (2019)			
		1024		512	
Multi-task learning	iCaRL Rebuffi et al. (2017)-SumLog Marra et al. (2019)	91.72	-4.28	90.32	-5.71
	iCaRL Marra et al. (2019)- SumLogit	93.19	-1.02	86.77	-10.09
	LUCIR Hou et al. (2019)- SumLogit	92.67	-2.34	91.88	-2.65

Table 9: Continual GANfake detection accuracies of the main evaluated methods on the GANfake dataset Marra et al. (2019) after the training on the last GAN using different memory budgets (1024 and 512).

buffi et al. (2017) and LUCIR Hou et al. (2019), while hurting the AA scores in the case of LRCIL Pellegrini et al. (2020) and CCIL Mittal et al. (2021).

Mixup. We further employ *Mixup* that is used a form of data augmentation for better clarification in general. The mixup technique is to generate training samples by linearly combining pairs of training samples (i.e., images and labels). Following Mittal et al. (2021), we applied the mixup data to the training data and merely used them (no original training data) to train the evaluated methods. It is interesting to see that mixup brings a clear performance degradation in the case of LRCIL. This is because the mixup operations are performed in the space of raw images, which is not consistent with learning mechanism of LRCIL that performs rehearsal in the latent space of feature maps. Except for LRCIL and CCIL*, the other two methods iCaRL, LUCIR favor the mixup technique for further improvement in terms of AA on the suggested CDDB.

A.3 EVALUATION ON THE GANFAKE DATASET

For the GANfake Marra et al. (2019) dataset⁴, Table 9 summarizes the evaluation results of the four main evaluated methods, i.e., the variant of iCaRL method Marra et al. (2019), our suggested SumLogit variants of LRCIL Pellegrini et al. (2020), iCaRL Rebuffi et al. (2017) and LUCIR Hou et al. (2019). The results show that the suggested MT variants mostly work better than the original

⁴Since the GANfake Marra et al. (2019) dataset does not release the detailed train/val/test splits, we can merely evaluate the methods on our own splits following the description in the original paper. Accordingly, the reported results are not really comparable with those reported in Marra et al. (2019).

one (i.e., SumLog). From the overall results, we can find that the highest AA score⁵ (i.e., 93.19) for the case of memory budget=1024 on GANfake is clearly higher than the one (i.e., 82.53) on our suggested CDDB-HARD1000 (memory budget=1000). Besides, the highest AA score (i.e., 91.88) for the case of memory size=512 on GANfake is much higher than the one (i.e., 80.77) on the suggested CDDB-HARD evaluation with memory budget = 500. Moreover, the highest AA score (i.e., 93.19) on GANfake (memory size=1024) is even higher than the one (i.e., 92.00) of our easiest evaluation, i.e., CDDB-EASY1500 (memory size=1500). This implies that our suggested CDDB is clearly more challenging than GANfake, and therefore it will have a high potential to promote more solid research in the domain of continual deepfake detection.

A.4 MORE OVERVIEWS OF FIVE CDDB EVALUATIONS

Fig.4 presents radar plots on the four evaluation metrics, i.e., AAs, AFs, mAPs and AA-Ms, of the evaluated methods for *EASY1500*, *LONG1500*, *HARD1500*, *HARD1000*, and *HARD500*, where 1500, 1000, 500 are three studied memory budgets, AA, AF, AA-M, mAP are Average Accuracy for deepfake detection, Average Forgetting degree, Average Accuracy for deepfake recognition, and mean Average Precision respectively. The mAP is calculated by the mean of areas under the precision-recall (PR) curves. For those multi-class and multi-task learning methods, we feed the PR calculation function with the normalized value of the maximum $\varphi(\cdot)$ activation output on fakes. Formally, the normalized value is $p_F = \frac{M_F}{M_F + M_R}$, where M_R and M_F are the maximum $\varphi(\cdot)$ activation values for reals and fakes respectively.

From the overall results in Fig.4, we can see that LUCIR-MT (multi-task learning) generally works the best than the other evaluated methods in terms of AA, AF, AA-M and mAP for the five evaluations. By comparing the five different evaluations, *HARD500*'s AA, AF, AA-M, mAP scores are clearly worse than the other four evaluations. This implies that the detection over *HARD500* is the most challenging. In particular, it suffers from much more serious catastrophic forgetting due to the smaller memory budget. Fig.5 presents the PR curves of the LUCIR method (with the highest mAP) for the five evaluations *EASY1500*, *LONG1500*, *HARD1500*, *HARD1000*, and *HARD500*. The five PR curves demonstrate that the most difficult tasks are the ones on SAN Dai et al. (2019), Wild-Deepfake Zi et al. (2020), and BigGAN Brock et al. (2019) for the five different evaluations. This is because SAN is a small data set, WildDeepfake consists of unknown deepfakes in the wild scenes, and BigGAN contains high-fidelity fakes of various classes.

⁵The reported highest AA is 97.22 in GANfake Marra et al. (2019) when the memory budget is 1024. It is even higher than our reported one, while their train/val/test splits in Marra et al. (2019) are different from ours.



Figure 4: Radar plots on AAs, AFs, mAPs and AA-Ms of the evaluated methods for *EASY1500* (top left), *LONG1500* (top right), *HARD1500* (middle), *HARD1000* (bottom left), and *HARD500* (bottom right), where 1500, 1000, 500 are memory budgets, BC/MC/MT: binary-class/multi-class/multi-task learning methods that have the highest AAs/mAPs, AA: Average Accuracy (detection), AF: Average Forgetting degree, AA-M: Average Accuracy (recognition), mAP: mean Average Precision, i.e., the mean of areas under the PR curve.

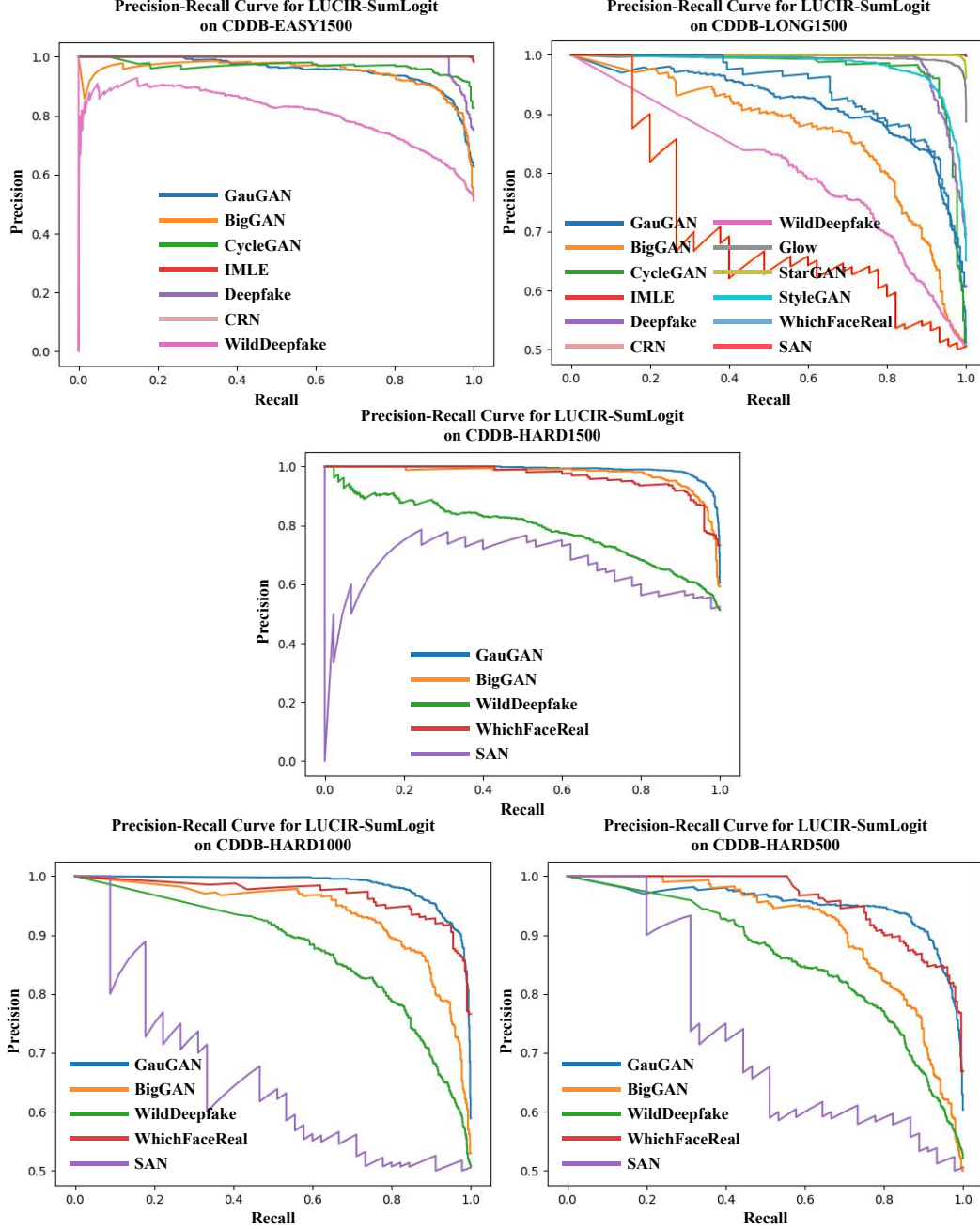


Figure 5: Precision-Recall (PR) curves of LUCIR-SumLogit with the highest mAP for the five CDDB evaluations *EASY1500* (top left), *LONG1500* (top right), *HARD1500* (middle), *HARD1000* (bottom left), and *HARD500* (bottom right), where 1500, 1000, 500 are memory budgets, and mAP is mean Average Precision, i.e., the mean of areas under all the PR curves.